Photonic Crystals

DOI: 10.1002/anie.201400686

Bio-Inspired Photonic-Crystal Microchip for Fluorescent Ultratrace Detection**

Jue Hou, Huacheng Zhang, Qiang Yang, Mingzhu Li, Yanlin Song,* and Lei Jiang*

Abstract: *Ultratrace detection attracts great interest because it is still a challenge to the early diagnosis and drug testing. Enriching the targets from highly diluted solutions to the sensitive area is a promising method. Inspired by the fog-collecting structure on Stenocara beetle's back, a photonic-crystal (PC) microchip with hydrophilic–hydrophobic micropattern was fabricated by inkjet printing. This device was used to realize high-sensitive ultratrace detection of fluorescence analytes and fluorophore-based assays. Coupled with the fluorescence enhancement effect of a PC, detection down to 10^{-16} mol L^{-1} was achieved. This design can be combined with biophotonic devices for the detection of drugs, diseases, and pollutions of the ecosystem.*

Ultratrace detection is of enormous interest in early diagnosis,[1] drugs testing,[2] explosives detection,[3] and eco-pollution determination.[4] The detection of analytes in highly diluted solution is a big challenge because detection is suffering from the weak signal and low signal-to-noise ratio (s/n) since the analytes are dispersed in too large volumes to be detected effectively. Enriching the targets from highly diluted solution to a sensitive area is a promising method to raise the concentration in a sensitive area to obtain a stronger signal and lower limit of detection.[5] The enrichment phenomenon widely exists in nature, such as the *Stenocara* beetle living in the desert,[6] which could effectively collect fog by a hydrophilic–hydrophobic pattern structure on its back. It provides an effective strategy to enrich target molecules from the highly diluted solution to the hydrophilic sensitive area by a wettability difference to effectively increase the sensitivity of molecule detection.

Photonic crystals (PCs), which are dielectric materials with periodic modulation of the refractive index and photonic band-gap properties,[7] have made possible sensitive detection of ions,[8] DNA,[9] proteins,[10] and other molecules[11] at comparatively low concentrations. Especially, based on the fluorescence enhancement effect, a PC device could achieve hundred-fold enhancement of sensitivity.[12] However, it is still a challenge to realize ultrasensitive detection at femto- or sub-femtomolar level.[9] A PC microchip combining fluorescence enhancement effect and enrichment ability of target molecules is predicted to realize ultratrace detection down to femto- or sub-femtomolar level.

Herein, we designed a PC microchip with a hydrophilic–hydrophobic micropattern to realize ultratrace and selective detection of analytes in highly diluted solution by enriching the analytes to hydrophilic active PC microsensor. This device realized highly sensitive ultratrace detection of fluorescence analytes and fluorophore-based assays down to 10^{-16} mol L^{-1} with a high s/n ratio (>10) and short accumulation time (100 ms). The detection limit was four orders of magnitude lower than that of a traditional PC chip. Moreover, this microchip was easy to manipulate, cost-effective, and robust. Our work provided a new strategy to realize ultratrace detection for analytes in highly diluted solution by combining the fluorescence enhancement and analyte enrichment.

As shown in Figure 1a, the scheme illustrated the fog-collecting structure on *Stenocara* beetle's back which could enrich tiny droplets from fog through the hydrophilic–hydrophobic micropattern. Inspired by such micropattern, a PC microchip with hydrophilic–hydrophobic micropattern was facilely fabricated by inkjet printing (Figure 1b) without expensive equipment or lithographic masks.[13] This PC microchip was printed by the hydrophilic monodispersed poly(styrene-methylmethacrylate-acrylic acid) (poly(St-MMA-AA)) spheres[14] on a hydrophobic polydimethylsiloxane (PDMS) substrate. All PC dots were about 200 μm in diameter. They were assembled from the monodispersed colloidal spheres with diameters of 180, 215, and 240 nm, named as PC_{180}, PC_{215}, and PC_{240}, respectively. They appeared blue (PC_{180}), green (PC_{215}), and red (PC_{240}) in color because of the Bragg scattering effect. A scanning electron microscope (SEM) image demonstrated that each PC dot was assembled as regular microplate (Figure 1c). The size and shape of the PC were well-controlled by the concentration of the colloidal spheres and the wettability of the substrate. To further fix the PC microplates onto the substrate, the PC-dotted PDMS was further cured after the assembly of the spheres. The optical properties of the PC dots were stable even when the

[*] Dr. J. Hou, Dr. H. Zhang, Dr. Q. Yang, Prof. Dr. M. Li, Prof. Dr. Y. Song, Prof. Dr. L. Jiang
Beijing National Laboratory for Molecular Science (BNLMS)
Key Laboratory of Green Printing
Key Laboratory of Organic Solids, Institute of Chemistry
Chinese Academy of Sciences, Beijing (P. R. China)
E-mail: mingzhu@iccas.ac.cn
ylsong@iccas.ac.cn
Homepage: http://ylsong.iccas.ac.cn
Dr. J. Hou, Dr. H. Zhang, Dr. Q. Yang
University of Chinese Academy of Sciences, Beijing (P. R. China)

[**] M.L. and Y.S. gratefully acknowledge financial support from the NSFC (grant numbers 51173190, 21003132, 91127038, and 21121001), the 973 Program (grant numbers 2013CB933004, 2011CB932303, and 2011CB808400), Beijing Nova Program (grant number Z131103000413051), and the "Strategic Priority Research Program" of the Chinese Academy of Sciences (grant number XDA09020000).

Supporting information for this article is available on the WWW under http://dx.doi.org/10.1002/anie.201400686.

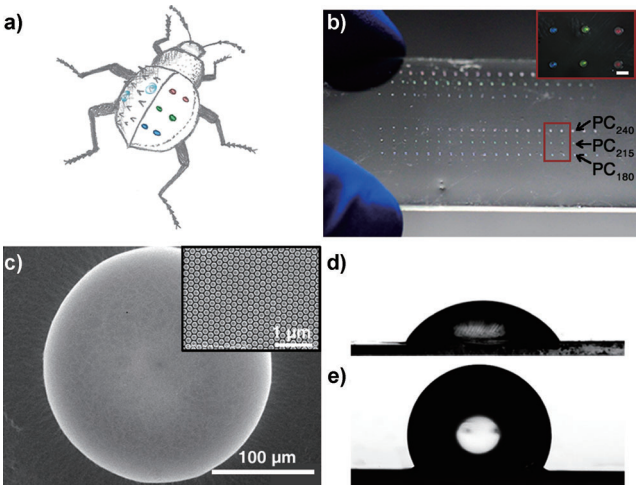

Figure 1. Bio-inspired PC microchip. a) The *Stenocara* beetle with hydrophilic–hydrophobic micropattern on the back for collecting water in fog. The colorful dot area represents the bio-inspired PC microchip. b) Photography of the bio-inspired PC microchip with hydrophilic PC dots on hydrophobic substrate. The inset shows the magnified picture corresponding to PC dots of different stopbands. The scale bar is 200 μm. c) SEM image of a PC dot. The inset shows the magnified SEM image of assembled colloidal spheres in the PC dot (the scale bar is 1 μm). d,e) Wettability difference between a PC dot (d, CA = 46.4 ± 3.4°) and a PDMS substrate (e, CA = 115.0 ± 3.1°).

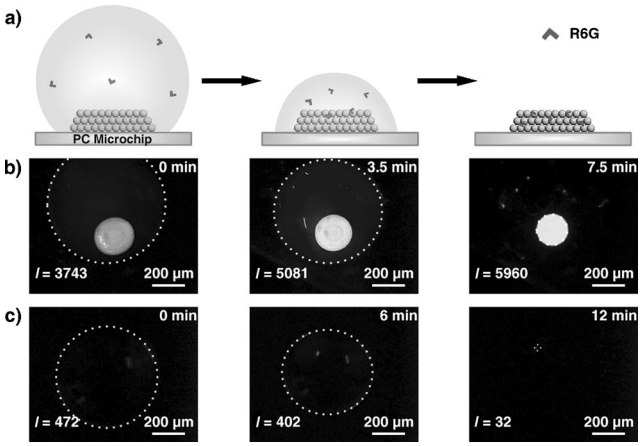

Figure 2. Enrichment process. a) The scheme and b) corresponding experimental images comprehensively illustrated the enrichment process of the fluorescence molecules (R6G) from the highly diluted solution droplet (0.5 μL, 10^{-10} mol L^{-1}) onto the PC dot. As the water evaporates, the concentration of R6G increases with the decreasing volume of the droplet, and the molecules are gradually enriched onto the PC dot, which induces fluorescence of the PC dot and the droplet area becomes brighter. Finally, all R6G molecules are enriched from the droplet to the PC dot and emit strongly. c) While on the superhydrophobic substrate which had the excellent enrichment ability, the intensity increased in the beginning and was then quenched because of the aggregation. The white circles show the edge of the drying droplet. *I* is the fluorescence intensity per pixel of the area of b) the PC dot and c) the droplet.

microchip was immersed in solutions of different pH values for one week (see Figure S1 in the Supporting Information). The contact angle (CA) of the PC dot was 46.4 ± 3.4° (Figure 1 d), whereas the CA of PDMS was 115.0 ± 3.1° (Figure 1 e). All PC dots had a highly ordered face-central-cubic structure and gave rise to high reflectivity (about 80 %) and narrow stopbands. The full-width-at-half-maxima of the stopbands were about 50 nm (Figure S2). This PC microchip could be exploited in detecting both fluorescence analytes and fluorophore-based assays which have been widely used in clinical diagnosis, drug testing, and eco-pollution determinations. For the fluorescence analyte highly diluted in aqueous solution, it could be detected directly by the PC microchip, and R6G solutions were used as examples. As fluorescence could be significantly enhanced at the band edges but suppressed inside gaps, the band structure of the PC was firstly optimized to achieve the highest enhancement of the R6G emission (Figure S2). PC_{215} with the stopband centered at 560 nm obtained the highest emission enhancement (46.4-fold), for its blue band-edge matched the emission wavelength and could remarkably enhance the spontaneous emission of the dye R6G sitting in the void of the PC matrix. Thus, the PC_{215} microchip was chosen to detect the R6G analyte.[15]

Figure 2 a shows the enrichment process of rare analytes from the highly diluted solution droplet onto the PC dot. The solution was dripped on the PC dot. Similar to the fog-collecting structure on *Stenocara* beetle's back, the droplet was pinned on the PC dot because of the wettability difference between the hydrophilic PC dot and the hydrophobic PDMS substrate. With the water evaporation, the solution dewetted from the hydrophobic substrate and was concentrated to the hydrophilic PC dot. Moreover, the PC was full of micropores so that the PC dot could absorb solution by capillarity like a sponge, which would benefit the enrichment.

Figure 2 b showed the enrichment process of R6G from the highly diluted solution droplet (0.5 μL, 10^{-10} mol L^{-1}) onto the PC dot. The droplet dried at 25 °C and 40 % relative humidity. The whole process was observed and recorded by fluorescence microscopy (Movie S1). At the beginning, the R6G droplet dripped on the PC microchip, and formed a 800 μm diameter hemisphere covering the PC dot (Figure 2 b, left). With the water evaporation, the analytes (R6G) were driven from the highly diluted solution to the sensitive area of the hydrophilic PC dot. The fluorescence intensity of the PC dot was rising. Finally, when all droplets completely dried, the maximal fluorescence intensity was obtained and the PC dot with the enriched R6G was bright and clearly observed in the fluorescent image.

Besides the hydrophilic–hydrophobic pattern inspired by the fog-collection effect of the *Stenocara* beetle, a superhydrophobic surface also has great ability in enriching the solution because of the self-cleaning effect inspired by the lotus surface.[16] Figure 2 c showed the enrichment process of R6G from the highly diluted solution droplet (0.5 μL, 10^{-10} mol L^{-1}) on the superhydrophobic surface. The superhydrophobic surface was made by coating the PDMS-modified silica nanoparticles solution (in chloroform) according to our previously reported method[17] and its CA was 160.8 ± 3.2°. The superhydrophobic substrate had excellent enrichment ability which could concentrate all the molecules into a tiny dot. As the droplet evaporated, pictures of

a brighter droplet were observed (Movie S2). But with more water evaporation and the further enrichment, the fluorescence then quenched. Finally, all molecules were driven and gathered together at an uncertain position of the superhydrophobic surface. The fluorescence intensity decreased to only 7% of the initial droplet. This was because aggregation-caused quenching (ACQ) effect occured when all dyes were driven and gathered together on the superhydrophobic surface. On the contrary, the PC dot provided a superior solid support for the dye molecules enrichment because the PC had large surface area and provided a superior sensitive area to disperse analytes, avoiding ACQ. Morever, this hydrophilic–hydrophobic micropattern could facilely drive and concentrate molecules towards the exact sensitive area.

To demonstrate the enrichment and enhancement ability of the PC microchip for R6G molecules, we systematically compared the fluorescence intensities of R6G (0.5 μL) at various concentrations from 10^{-4} to 10^{-16} mol L^{-1} on different substrates: hydrophilic glass, hydrophobic PDMS, hydrophilic PC film, and PC microchip. Figure 3 showed fluorescence

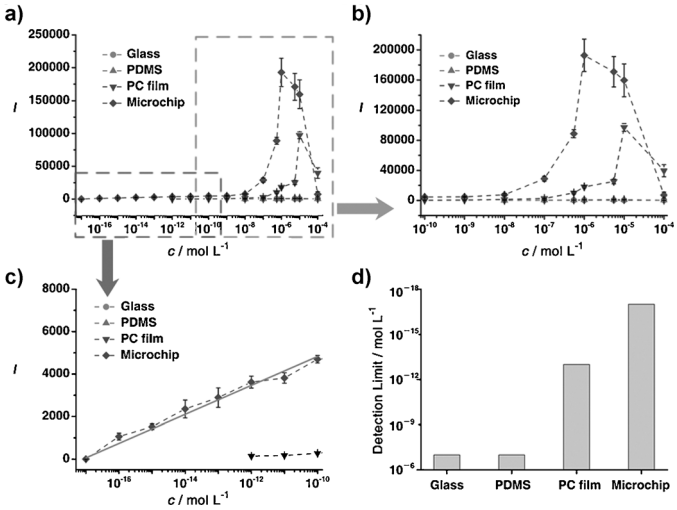

Figure 3. Detection of R6G. a) Fluorescence intensities of R6G at different concentrations (10^{-4} to 10^{-16} mol L^{-1}) on different substrates. b,c) Enlarged illustrations of the fluorescence intensities in high concentration (b, 10^{-4} to 10^{-10} mol L^{-1}) and low concentration (c, 10^{-10} to 10^{-16} mol L^{-1}) of (a). The red line in (c) was the simulation of the fluorescence intensity on the PC microchip at concentrations from 10^{-10} to 10^{-16} mol L^{-1}. d) Detection limits of different substrates. The PC microchip achieved the lowest detection limit.

intensities of R6G at different concentrations on different substrates. Each point was averaged from at least ten independent measurements. It clearly showed that the PC microchip had the best performance in the fluorescence molecule detection due to the combination of the enrichment ability of hydrophilic–hydrophobic micropattern and the fluorescence enhancement effect of the PC. The PC film with the stopband centered at 560 nm was the better one. The PC_{215} still significantly enhanced the spontaneous emission of the R6G emission when the dye molecules were driven to the PC matrix with the solution evaporation, although the droplet spread widely on the surface. On the glass and PDMS substrate, the R6G emission was weak because these two subatrates had neither effective enrichment nor fluorescence enhancement ability.

At high concentrations from 10^{-4} to 10^{-10} mol L^{-1} (Figure 3b), all four substrates had similar tendency that the fluorescence increased firstly with increasing concentration of R6G, and then quenched at certain concentration when the concentration induced ACQ. The quenching concentrations of the glass, PDMS, PC film and PC microchip were 5×10^{-6}, 5×10^{-6}, 1×10^{-5}, and 1×10^{-6} mol L^{-1}, respectively. The quenching concentration of the PC microchip was the lowest which indicated the PC microchip had the best enrichment ability among these substrates. At low concentration from 10^{-10} to 10^{-16} mol L^{-1} (Figure 3c), the fluorescence intensities of R6G could be detected only on PC film and PC microchip. The R6G emissions on the other substrates were hardly detected until the concentration of R6G reached 10^{-8} mol L^{-1}. On the PC microchip, the fluorescence signal at 10^{-16} mol L^{-1} was strong enough to be detected with high s/n (100 s/n). On the PC film, the signal was merged in the noise and could not be read out at a concentration lower than 10^{-12} mol L^{-1}. As shown in the Figure 3c (gray solid line), the corresponding calibration plot of emission intensity (I) versus the logarithm of R6G concentration was linear at low concentration region (C, 1×10^{-10} to 1×10^{-16} mol L^{-1}). The regression equation of the detection assisted by PC microchip was $I = 684\lg[C] + 11645$, with a correlation coefficient of 0.9964. The detection limits of the glass, PDMS, PC film, and PC microchip were accordingly 1.3×10^{-8}, 1.2×10^{-8}, 6.5×10^{-13}, and 1.4×10^{-17} mol L^{-1} (Figure 3d). The detection limits of glass and PDMS were at same level. The PC film lowered the detection limit about five orders of magnitude relative to glass because of its fluorescence enhancement effect. The PC microchip lowered the detection limit by four orders of magnitude relative to the traditional PC film and the fluorescence intensity was greatly enhanced because all R6G molecules were enriched in the sensitive PC area and excited effectively. Compared with the detection on glass, the PC microchip lowered the detection limit by nine orders of magnitude, which confirmed the great ablility of the PC microchip for the enrichment and fluorescence enhancement.

This PC microchip is universal for fluorophore-based assays and could be combine with existing fluorescent analysis system to realize ultratrace detection. Herein, a fluorophore-labeled aptamer for cocaine was used to demonstrate the universal ability of the prepared PC microchip. The estimates of the amounts of cocaine manufactured, expressed in quantities of 100% pure cocaine, ranged from 776 to 1051 tons in 2011, as one of the main addictive drug.[18] To face the appearance of new drugs camouflages, comparatively fast and high-sensitive detection methods were recently reported to detect samples at low concentration.[19] Shi et al.[20] developed a rolling circle amplification and magnitud-enrich method, and realized the lowest cocaine detection at 4.8×10^{-10} mol L^{-1}. However, high-sensitive detection of cocaine is still a big challenge. To detect cocaine by

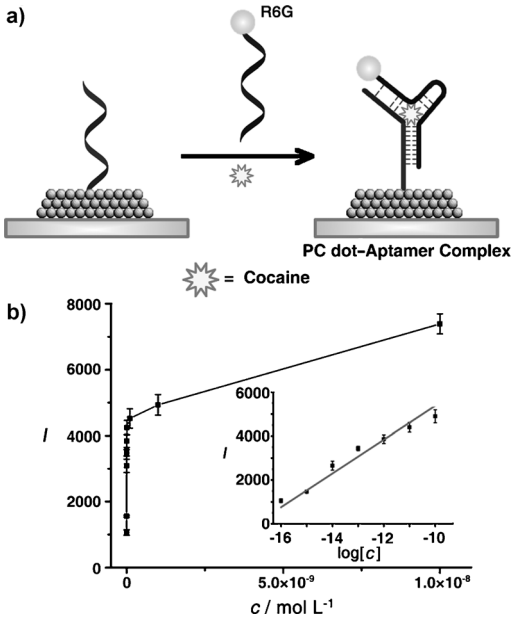

Figure 4. Cocaine detection with a DNA-aptamer-modified PC microchip. a) Schematic representation of the cocaine detection mechanism: Capture DNA was first used to functionalize the PC dot. Then cocaine could be indirectly detected by enriching the cocaine molecules and the R6G-labeled target DNA from solution onto the PC dot to form a PC dot–aptamer complex. b) The fluorescence intensities at different cocaine concentrations. The inset shows a linear relationship between fluorescence intensity and the logarithm of the cocaine concentration (1×10^{-10} to 1×10^{-16} mol L^{-1}).

a fluorescence method, we combined the aptamer-based method[21] with our PC microchip to further increase the detection sensitivity of cocaine. As shown in Figure 4, cocaine was enriched on the PC dot and specifically captured by a DNA-functionalized PC dot and R6G-labeled target DNA, realized fluorescence detection. (The detail of the experiment is given in the Experimental Section of Supporting Information.) The detection limit was 1.4×10^{-17} mol L^{-1}, which was the lowest in cocaine detection.

In summary, inspired by fog-collecting structure of *Stenocara* beetle, we fabricated a PC microchip with hydrophilic–hydrophobic micropattern and exploited it in detections of fluorescence analytes and molecular fluorephore-based assays. The wettability difference in water contact angles between the hydrophilic PC dot and hydrophobic substrate induced the target molecules to enrich the active PC microsensors. Ultratrace detections of fluorescence analyte (R6G) and molecular fluorephore-based assays (cocaine) down to 10^{-16} mol L^{-1} were achieved. This PC microchip is stable, high-sensitive, robust, and cost-effective. Our work provides a new strategy to lower the detection limit by four orders of magnitude compared with the traditional PC chip. It might be coupled with aptamer technology and immunofluorescence technique and used to realize high-throughput and ultrasensitive detection in clinical diagnosis and life science.

Received: January 22, 2014
Published online: March 28, 2014

Keywords: cocaine · enrichment · fluorescence enhancement · photonic crystals · ultratrace detection

[1] a) S. K. Arya, S. Bhansali, *Chem. Rev.* **2011**, *111*, 6783 – 6809; b) F. S. Apple, S. W. Smith, L. A. Pearce, R. Ler, M. M. Murakami, *Clin. Chem.* **2008**, *54*, 723 – 728.
[2] a) T. A. Brettell, J. M. Butler, J. R. Almirall, *Anal. Chem.* **2007**, *79*, 4365 – 4384; b) T. A. Brettell, J. M. Butler, J. R. Almirall, *Anal. Chem.* **2011**, *83*, 4539 – 4556; c) P. López, A. M. Bermejo, M. J. Tabernero, P. Cabarcos, I. Álvarez, P. Fernández, *J. Anal. Toxicol.* **2009**, *33*, 351 – 355.
[3] a) J. I. Steinfeld, J. Wormhoudt, *Annu. Rev. Phys. Chem.* **1998**, *49*, 203 – 232; b) Y. Engel, R. Elnathan, A. Pevzner, G. Davidi, E. Flaxer, F. Patolsky, *Angew. Chem.* **2010**, *122*, 6982 – 6987; *Angew. Chem. Int. Ed.* **2010**, *49*, 6830 – 6835; c) H. X. Zhang, J. S. Hu, C. J. Yan, L. Jiang, L. J. Wan, *Phys. Chem. Chem. Phys.* **2006**, *8*, 3567 – 3572.
[4] a) E. M. Nolan, S. J. Lippard, *Chem. Rev.* **2008**, *108*, 3443 – 3480; b) E. Rodríguez, F. Navarro-Villoslada, E. Benito-Peña, M. D. Marazuela, M. C. Moreno-Bondi, *Anal. Chem.* **2011**, *83*, 2046 – 2055.
[5] a) J. Gao, H. Gu, B. Xu, *Acc. Chem. Res.* **2009**, *42*, 1097 – 1107; b) S. D. Soelberg, R. C. Stevens, A. P. Limaye, C. E. Furlong, *Anal. Chem.* **2009**, *81*, 2357 – 2363; c) F. De Angelis, F. Gentile, F. Mecarini, G. Das, M. Moretti, P. Candeloro, M. L. Coluccio, G. Cojoc, A. Accardo, C. Liberale, R. P. Zaccaria, G. Perozziello, L. Tirinato, A. Toma, G. Cuda, R. Cingolani, E. Di Fabrizio, *Nat. Photonics* **2011**, *5*, 682 – 687.
[6] A. R. Parker, C. R. Lawrence, *Nature* **2001**, *414*, 33 – 34.
[7] a) E. Yablonovitch, *Phys. Rev. Lett.* **1987**, *58*, 2059 – 2062; b) S. John, *Phys. Rev. Lett.* **1987**, *58*, 2486 – 2489; c) L. He, M. Wang, J. Ge, Y. Yin, *Acc. Chem. Res.* **2012**, *45*, 1431 – 1440.
[8] a) J. H. Holtz, S. A. Asher, *Nature* **1997**, *389*, 829 – 832; b) J. Ge, J. Goebl, L. He, Z. Lu, Y. Yin, *Adv. Mater.* **2009**, *21*, 4259 – 4264; c) B. F. Ye, Y. J. Zhao, Y. Cheng, T. T. Li, Z. Y. Xie, X. W. Zhao, Z. Z. Gu, *Nanoscale* **2012**, *4*, 5998 – 6003; d) Y. Huang, F. Li, M. Qin, L. Jiang, Y. Song, *Angew. Chem.* **2013**, *125*, 7437 – 7440; *Angew. Chem. Int. Ed.* **2013**, *52*, 7296 – 7299.
[9] M. Li, F. He, Q. Liao, J. Liu, L. Xu, L. Jiang, Y. Song, S. Wang, D. Zhu, *Angew. Chem.* **2008**, *120*, 7368 – 7372; *Angew. Chem. Int. Ed.* **2008**, *47*, 7258 – 7262.
[10] a) Y. J. Zhao, X. W. Zhao, J. Hu, J. Li, W. Y. Xu, Z. Z. Gu, *Angew. Chem.* **2009**, *121*, 7486 – 7488; *Angew. Chem. Int. Ed.* **2009**, *48*, 7350 – 7352; b) S. Mandal, J. M. Goddard, D. Erickson, *Lab Chip* **2009**, *9*, 2924 – 2932; c) Y. J. Zhao, X. W. Zhao, Z. Z. Gu, *Adv. Funct. Mater.* **2010**, *20*, 2970 – 2988.
[11] a) S. A. Asher, V. L. Alexeev, A. V. Goponenko, A. C. Sharma, I. K. Lednev, C. S. Wilcox, D. N. Finegold, *J. Am. Chem. Soc.* **2003**, *125*, 3322 – 3329; b) H. Fudouzi, Y. Xia, *Adv. Mater.* **2003**, *15*, 892 – 896; c) X. Xu, A. V. Goponenko, S. A. Asher, *J. Am. Chem. Soc.* **2008**, *130*, 3113 – 3119; d) H. Li, J. X. Wang, Z. L. Pan, L. Y. Cui, L. A. Xu, R. M. Wang, Y. L. Song, L. Jiang, *J. Mater. Chem.* **2011**, *21*, 1730 – 1735; e) J. Ge, Y. Yin, *Angew. Chem.* **2011**, *123*, 1530 – 1561; *Angew. Chem. Int. Ed.* **2011**, *50*, 1492 – 1522; f) I. B. Burgess, L. Mishchenko, B. D. Hatton, M. Kolle, M. Loncar, J. Aizenberg, *J. Am. Chem. Soc.* **2011**, *133*, 12430 – 12432.
[12] a) N. Ganesh, W. Zhang, P. C. Mathias, E. Chow, J. A. N. T. Soares, V. Malyarchuk, A. D. Smith, B. T. Cunningham, *Nat. Nanotechnol.* **2007**, *2*, 515 – 520; b) W. Shen, M. Li, L. Xu, S. Wang, L. Jiang, Y. Song, D. Zhu, *Biosens. Bioelectron.* **2011**, *26*, 2165 – 2170.
[13] W. Shen, M. Li, C. Ye, L. Jiang, Y. Song, *Lab Chip* **2012**, *12*, 3089 – 3095.
[14] J. X. Wang, Y. Q. Wen, H. L. Ge, Z. W. Sun, Y. M. Zheng, Y. L. Song, L. Jiang, *Macromol. Chem. Phys.* **2006**, *207*, 596 – 604.

[15] a) S. Nishimura, N. Abrams, B. A. Lewis, L. I. Halaoui, T. E. Mallouk, K. D. Benkstein, J. van de Lagemaat, A. J. Frank, *J. Am. Chem. Soc.* **2003**, *125*, 6306 – 6310; b) A. F. Koenderink, W. L. Vos, *Phys. Rev. Lett.* **2003**, *91*, 213902; c) G. von Freymann, S. John, S. Wong, V. Kitaev, G. A. Ozin, *Appl. Phys. Lett.* **2005**, *86*, 053108; d) G. von Freymann, S. John, V. Kitaev, G. A. Ozin, *Adv. Mater.* **2005**, *17*, 1273 – 1276; e) L. Bechger, P. Lodahl, W. L. Vos, *J. Phys. Chem. B* **2005**, *109*, 9980 – 9988; f) J. I. L. Chen, G. von Freymann, S. Y. Choi, V. Kitaev, G. A. Ozin, *J. Mater. Chem.* **2008**, *18*, 369 – 373; g) C. Blum, A. P. Mosk, I. S. Nikolaev, V. Subramaniam, W. L. Vos, *Small* **2008**, *4*, 492 – 496.

[16] a) L. Feng, S. H. Li, Y. S. Li, H. J. Li, L. J. Zhang, J. Zhai, Y. L. Song, B. Q. Liu, L. Jiang, D. B. Zhu, *Adv. Mater.* **2002**, *14*, 1857 – 1860; b) T. Sun, L. Feng, X. Gao, L. Jiang, *Acc. Chem. Res.* **2005**, *38*, 644 – 652; c) T. Sun, G. Qing, B. Su, L. Jiang, *Chem. Soc. Rev.* **2011**, *40*, 2909 – 2921.

[17] Y. Huang, J. Zhou, B. Su, L. Shi, J. Wang, S. Chen, L. Wang, J. Zi, Y. Song, L. Jiang, *J. Am. Chem. Soc.* **2012**, *134*, 17053 – 17058.

[18] UNODC, *World Drug Report 2013*, United Nations, **2013**.

[19] a) M. N. Stojanovic, P. de Prada, D. W. Landry, *J. Am. Chem. Soc.* **2001**, *123*, 4928 – 4931; b) M. N. Stojanovic, D. W. Landry, *J. Am. Chem. Soc.* **2002**, *124*, 9678 – 9679; c) B. R. Baker, R. Y. Lai, M. S. Wood, E. H. Doctor, A. J. Heeger, K. W. Plaxco, *J. Am. Chem. Soc.* **2006**, *128*, 3138 – 3139; d) J. W. Liu, Y. Lu, *Angew. Chem.* **2006**, *118*, 96 – 100; *Angew. Chem. Int. Ed.* **2006**, *45*, 90 – 94; e) C. Y. Zhang, L. W. Johnson, *Anal. Chem.* **2009**, *81*, 3051 – 3055; f) J. L. He, Z. S. Wu, H. Zhou, H. Q. Wang, J. H. Jiang, G. L. Shen, R. Q. Yu, *Anal. Chem.* **2010**, *82*, 1358 – 1364.

[20] C. Ma, W. Wang, Q. Yang, C. Shi, L. Cao, *Biosens. Bioelectron.* **2011**, *26*, 3309 – 3312.

[21] E. Golub, G. Pelossof, R. Freeman, H. Zhang, I. Willner, *Anal. Chem.* **2009**, *81*, 9291 – 9298.

